International Journal of Nanomedicine

Dovepress

open access to scientific and medical research

Open Access Full Text Article

ORIGINAL RESEARCH

Exosome Derived from Mesenchymal Stem Cells Alleviates Pathological Scars by Inhibiting the Proliferation, Migration and Protein Expression of Fibroblasts via Delivering miR-138-5p to Target SIRT1

Wen Zhao[1], Rui Zhang[1], Chengyu Zang[1], Linfeng Zhang[1], Ran Zhao[1], Qiuchen Li[1], Zhanjie Yang[1], Zhang Feng[1], Wei Zhang[1], Rongtao Cui[1,2]

[1]Department of Burn and Plastic Surgery, Shandong Provincial Hospital Affiliated to Shandong First Medical University, Jinan, People's Republic of China; [2]Department of Burn and Plastic Surgery, Shandong Provincial Hospital, Cheeloo College of Medicine, Shandong University, Jinan, People's Republic of China

Correspondence: Rongtao Cui, Department of Burn and Plastic Surgery, Shandong Provincial Hospital Affiliated to Shandong First Medical University, Jinan, People's Republic of China, Tel +86 18653170822, Email cuirt1986@outlook.com

Introduction: The therapies of using exosomes derived from mesenchymal stem cells (MSC-Exo) for wound healing and scar attenuation and micro RNAs (miRNAs) for regulation of genes by translational inhibition and mRNA destabilization obtained great achievements. Silent information regulator 1 (SIRT1) is the silent information, which has an intricate role in many biological processes. However, the effects of SIRT1 and miR-138-5p loaded in MSC-Exo on pathological scars remain unclear.

Methods: MSC-Exo was isolated and identified by ultracentrifugation, transmission electron microscopy, nanoparticle size measuring instrument and Western blot assays. The relationship between SIRT1 and miR-138-5p was verified by a double-luciferase reporter assay. Cell Counting Kit-8, Transwell, scratch, and Western blot assays were used to evaluate the proliferation and migration of human skin fibroblasts (HSFs), and the protein expression of SIRT1, NF-κB, α-SMA and TGF-β1 in HSFs, respectively. Flow cytometry was used to assess the apoptosis and cell cycle of HSFs affected by SIRT1.

Results: Our study demonstrated that miR-138-5p loaded in MSC-Exo could attenuate proliferation, migration and protein expression of HSFs-derived NF-κB, α-SMA, and TGF-β1 by targeting to SIRT1 gene, which confirmed the potential effects of MSC-Exo in alleviating pathological scars by performing as a miRNA's delivery vehicle.

Conclusion: Exosomes derived from MSCs acting as a delivery vehicle to deliver miR-138-5p can downregulate SIRT1 to inhibit the growth and protein expression of HSFs and attenuate pathological scars.

Keywords: mesenchymal stem cell-derived exosomes, miR-138-5p, SIRT1, human skin fibroblasts, pathological scars

Introduction

Pathological scars, mainly including hypertrophic scars (HS) and keloids, are hyperplasia of human skin fibroblasts (HSFs) that result from injury to the skin.[1] The complications caused by HS and keloids, such as pain, pruritus, burning, paresthesia, etc., affect patients both physiologically and psychologically.[2] Many studies have been on HS and keloids, but the mechanisms underlying scar formation have not yet been well established, and prophylactic and treatment strategies remain unsatisfactory. Whereas what is clear is that the fibroblast-induced fibrosis and inflammation play a pivotal role in cutaneous scarring.[2–4]

Mesenchymal stem cells (MSCs) release exosomes, which are tiny (30–150 nm in diameter) external membrane vesicles with proteins and nucleic acids. Exosomes not only have the same effects as MSCs but also have the benefits of

Received: 15 June 2022
Accepted: 1 September 2022
Published: 8 September 2022

targeted administration, minimal immunogenicity, and high repairability.[5–8] The main function of mesenchymal stem cell-derived exosomes (MSC-Exo) is in cell communication where they deliver cell-type-specific proteins and nucleic acids, including mRNAs, miRNAs and lncRNAs, to regulate target genes.[9,10] Ha et al[11] reported that MSC-Exo could be an effective therapeutic for skin regeneration by immunomodulatory. An et al[8] summarized that exosomes derived from adipose-derived stem cells (ADSC-Exo) modulate immune responses and inflammation during wound healing, which could also promote angiogenesis, accelerate proliferation and re-epithelization of skin cells, regulate collagen remodeling and inhibit scar hyperplasia. Fang et al[12] demonstrated that umbilical cord MSCs-derived exosomes (uMSC-Exo) reduced scar formation and myofibroblast accumulation in a skin-defect mouse model, which was mainly dependent on exosomal microRNAs (miRNAs). These previous studies all confirmed the promising roles of MSC-Exo in wound healing and scar alleviation through immunomodulation, angiogenesis, re-epithelization and remodeling.[13]

miRNAs are small non-coding RNAs that play important role in scarring through posttranscriptional gene regulation by translational inhibition and mRNA destabilization.[14] It inhibits the translation of genes and downregulates target gene expressions by binding to the 3′-untranslated regions (3′-UTRs) of mRNAs.[15] The ability of miRNAs to control the factors and pathways leading to fibrosis could lead to the development of therapeutic agents. Several recent developments in this area have involved the use of miRNAs.[16–18] However, there are difficulties in delivering miRNAs to cellular models.[19,20] Therefore, the use of exosomes provides an effective way for miRNAs delivery. Furthermore, previous studies demonstrated that miR-138-5p could inhibit the progression of cancers by suppressing the proliferation, growth, and migration of cancer cells, indicating that miR-138-5p may be a cancer-related miRNA.[21–23] Another study showed that circ_101238/miR-138-5p/CDK6 signaling axis could inhibit cell proliferation while promoting apoptosis of keloid fibroblasts.[24] Therefore, miR-138-5p may play a pivotal role in therapeutics for tumorous and fibrotic diseases, which still needs further exploration.

As we all know, silent information regulator 1 (SIRT1) is a ubiquitously expressed protein and an NAD^+-dependent deacetylase that regulates gene expression by histone deacetylation.[25] SIRT1 has an intricate role in the processes of reactive oxygen species (ROS), inflammatory response, fibrosis, apoptosis, epithelial-to-mesenchymal transition, and treatment of several diseases.[25–28] The literature survey on the deletion of SIRT1 shows evidence for its effects in preventing oxidative stress, inflammation, as well as fibrosis.[26,29] Uncertainty persists regarding SIRT1′s impact on HSFs and its underlying regulatory system. Contrarily, in our early tests, we found that SIRT1 elevated the expression of inflammatory and profibrotic proteins in HSFs, promoted the proliferation and migration of HSFs, and supported the role of SIRT1 in inducing skin fibrosis. As a result, we suggest that SIRT1 may play a role in the regulatory process that controls the growth and development of pathological scars. Is there a relationship between SIRT1 and miR-138-5p in HSFs, though?

Therefore, our present study investigated the functional changes of HSFs under influence of SIRT1 and miR-138-5p loaded in MSC-Exo through the HSFs model in vitro.

Methods

Cell Culture

Cell culture was performed by referring to previous studies.[30,31] HSFs (FuHeng BioLogy, Shanghai, China), derived from scar tissue, were cultured with DMEM (Gibco, NY, USA) supplemented with 10% FBS (Gibco, NY, USA), 100U/mL penicillin, and 100μg/mL streptomycin in a humidified incubator containing 5% (v/v) CO_2 at 37 °C. When the HSFs reached 90% confluence, the HSFs were subcultured. HSFs from the third to the fifth passages were used for subsequent experiments. HSFs were cultured in six-well plates at a concentration of 1.5×10^5 cells/well, starved in serum-free medium overnight when grown to 70~80% confluent, and then stimulated with SIRT1 overexpression or knockdown, MSC-Exo (20μg/mL), miR-138-5p loaded in MSC-Exo (20μg/mL), miRNAs mimics (100nM), inhibitors (100nM) and negative control (100nM) that transfected with Lipofectamine®2000 reagent (Life Technologies Invitrogen, Carlsbad, CA, USA) for approximately 24 h or 48 h to detect the protein levels, or proliferation, migration, cell cycle and apoptosis of HSFs. The lysates were used to analyze the expression of exosome markers (CD9, CD81, and TSG101).

The Isolation of MSC-Exo

Exosomes were isolated from the collected medium by differential ultracentrifugation.[7,32] The cell-conditioned medium was collected from approximately 70% confluent MSCs (Cyagen, China) at a concentration of 6×10^5 cells/well grown in 100-mm cell culture dishes with 10mL human MSC basal medium containing FBS depleted of bovine serum extracellular vesicles (JKF1001-100, QIAGEN, Shandong, China) in each dish by 48~36 h. About 1000mL of cell supernatant was collected, and 100mL of cell supernatant was firstly centrifuged at 2000 ×*g* for 15min to remove dead cells. Next, the supernatant was centrifuged at 10,000 ×*g* for 30 minutes to remove impurities. Then, the supernatant was centrifuged at 120,000 ×*g* for 70 minutes using a Ti70 rotor (Optima XPN-100 Ultracentrifuge, Beckman Coulter, Kraemer Boulevard Brea, USA). All centrifugation steps were performed at 4 °C. Eventually, exosomes were isolated from the collected medium by differential ultracentrifugation.

Lentivirus Transfection

The SIRT1 knockdown and SIRT1 overexpressing lentiviruses were purchased from the Oligobio company (Beijing, China). The specific sequences of human SIRT1 small interfering RNA and miRNA mimics or miRNA-inhibitor mimics used were as follows:

Si-RNA

Small interfering RNA SIRT1: 5′-GGGUCUUCCCUCAAAGUAATT-3′.
Negative control: 5′-TTCTCCGAACGTGTCACGTTT-3′.

miRNA Mimics

miR-138-5p mimics: 5′-AGCUGGUGUUGUGAAUCAGGCCG-3′
miR-181a-5p mimics: 5′-AACAUUCAACGCUGUCGGUGAGU-3′
miR-524-5p mimics: 5′-CUACAAAGGGAAGCACUUUCUC-3′
miR-601 mimics: 5′-UGGUCUAGGAUUGUUGGAGGAG-3′
miR-1283 mimics: 5′-UCUACAAAGGAAAGCGCUUUCU-3′
Negative control: 5′-UUGUACUACACAAAAGUACUG-3′.

miRNA-Inhibitor Mimics

miR-138-5p-inhibitor mimics: 5′-CGGCCUGAUUCACAACACCAGCU-3′
Negative control: 5′-CAGUACUUUUGUGUAGUACAA-3′.

Lentivirus transfection was performed by referring to a previous study.[30] HSFs (1×10^5 cells/well) were grown in six-well plates, and the appropriate lentivirus (multiplicity of infection = 20) was added to the wells. Twenty-four hours later, the medium containing the lentivirus was discarded and replaced with 2mL fresh medium. After 72 h transfection, HSFs were subjected to puromycin for one week to select stably infected cells. All transfections were performed in triplicate.

Western Blot Assays

Western blot assays were performed by referring to previous studies.[7,30,31] HSFs were collected, washed twice with ice-cold PBS to extract cellular proteins, and digested with trypsin. Lysed samples were incubated on ice for 30 min. Cell lysates were then centrifuged at 12,000 ×*g* at 4 °C for 5 min to remove cellular debris. Briefly, 50μg of total protein were subjected to 10% SDS-PAGE gels (Tanon, Shanghai, China) and loaded the prepared sample to conduct electrophoresis under the constant voltage 80V for 2 h and transferred to PVDF Transfer Membranes (Tanon, Shanghai, China) by using a transfer electrophoresis device under the condition of 4°C, 300mA constant current for 150 min. Then, membranes were blocked for 3 h in 5% non-fat dry milk in TBST solution, containing 5% skimmed milk, at room temperature, then incubated with primary antibodies specific to SIRT1 (1:1000, CST, USA), NF-κB (1:2000, Proteintech, USA), α-SMA (1:5000, Proteintech, USA), TGF-β1 (1:1000, Proteintech, USA), CD9, CD81, TSG101 (1:1000, Proteintech, USA), and GAPDH (1:5000, Proteintech, USA) at 4 °C overnight. The next day, the membranes were incubated with HRP-conjugated anti-rabbit IgG secondary antibodies (1:5000, Affinity, USA) at 37 °C for 1 h. For chemiluminescence detection of proteins, immunoreactive traces on the membrane were visualized with ECL Kit (RPN2232, Amersham,

USA) on a FluorChem FC system (Alpha Innotech, ProteinSimple, USA), and the intensity of protein expression was analyzed by ImageJ software and normalized against GAPDH.

Cell Counting Kit-8 Assays

Cell Counting Kit-8 assays were performed by referring to previous studies.[30,31] The Cell Counting Kit-8 (MedChemExpress, USA) assay was used to measure cell proliferation. Take 9×10^5 cells from each group and resuspended by 3mL complete medium. The different group cells were seeded in 96-well plates with 100μL of cell suspension and cultured for 0-, 24-, 48-, 72-, and 96-hour time points. Ten microliters of the Cell Counting Kit-8 reagent were added to each well and incubated for one and half hours. The absorbance at 450 nm was measured using a microplate reader (Infinite F50, TECAN, Switzerland).

Scratch Assays

Scratch assays were performed by referring to previous studies.[7,30,31] The scratch wound assay was used to evaluate the migration of different group cells. The cells were seeded in 24-well plates at a density of 1.5×10^5 cells/well and cultured until they reached approximately 100% confluence. A scratch wound was generated on the cells' surface by 1 mL pipette tips. PBS was used to remove the floating cells, then changed to a serum-free medium and put in a humidified incubator containing 5% (v/v) CO_2 at 37 °C. Digital images of each scratch distance at 0-, 24-hour time points were captured. Using ImageJ software to count the number of migrated cells.

Transwell Migration Assays

Transwell migration assays were performed by referring to previous studies.[7,30,31] The upper chamber of a 24-well transwell plate with an 8μm aperture of the filter membrane (3422, Corning, NY, USA) was filled with 100μL of complete medium containing FBS, and 100μL cell suspension of HSFs was seeded at a density of 5×10^4 cells/well. About 600μL of cultured supplemented with SIRT1 overexpression or knockdown, miRNAs mimics or inhibitors, MSC-Exo, miR-138-5p modified MSC-Exo, and their negative controls or an equal volume of FBS were added to the lower chamber and incubated for 24 h. Then, HSFs were fixed with 4% paraformaldehyde for 30 min and washed with PBS three times. HSFs were dyed with 400μL of 0.5% crystal violet staining solution (Boster, Wuhan, China) and incubated for 30 min at room temperature. After washing with PBS, the number of migrated cells was observed under a microscope (CKX-51, Olympus, Tokyo, Japan).

Flow Cytometry

Flow cytometry was performed by referring to a previous study.[7] The different groups of cells were spread in six-well cell culture plates and then were digested with 0.25% trypsin and subjected to centrifuge at 1500 rpm for 5 min. Each group was repeated with three multiple wells. Then, the pellets were washed with PBS, cautiously added, dropwise with precooled 70% ethanol to make HSFs be fixed uniformly. HSFs were cryopreserved at −20 °C overnight. Thereafter, HSFs were washed with PBS three times at 1500 rpm for 10 min, resuspended with 500μL of PI/Rnase staining (FACSCalibur, BD, USA), and incubated in dark places for 15 min at room temperature. The percentage of cell cycle in each phase and cell apoptosis were detected by using BD Accuri™ C6 flow cytometer.

Dual-Luciferase Assays

Dual-Luciferase Assays were performed by referring to previous studies.[7] To ensure that SIRT1 was indeed a direct target of miR-138-5p, we obtained luciferase-3′-untranslated region (3′-UTR) reporter constructs of SIRT1 mRNA (Promega, WI, USA). Co-transfections of wild-type SIRT1 3′-UTR, mutant SIRT1 3′-UTR, or their non-targeting control RNA with miR-138-5p mimics at a final concentration of 50nM were accomplished with Lipofectamine®2000 transfection reagent. The samples were harvested after 48h for luciferase assays.

The Identification and Label of MSC-Exo

The identification and label of MSC-Exo were performed by referring to previous studies.[7,32] About 10μL of isolated exosomes were resuspended in 200μL PBS, the morphology of isolated exosomes was immediately visualized by transmission electron microscope (TEM; HT7800, Hitachi), and the distribution of size was analyzed by nanoparticle tracking analysis (NTA; Particle Metrix, ZetaView PMX110). Meanwhile, immunoblotting was performed to detect the expression of known exosomal markers CD9, CD81, and TSG101. Exosome diluted in culture medium was passed through a 0.22-μm filter to keep sterilized before the experiment started. The extra exosome precipitation was redissolved with PBS and stored at −80°C for standby. The purified exosome was labeled with fluorescence using a PKH67 kit (MIDI67-1KT, Sigma, St. Louis, USA). Take 200μL of dilute C solution in PKH67 kit and blow repeatedly to fully resuspend the precipitation of secretion; take 200μL of dilute C solution in PKH67 kit and add 2μL of PKH67 dye solution then mix well. Mix the A and B solution evenly, incubate at room temperature for 5 min and keep away from light. Add 400μL of 10% BSA-PBS solution to stop dyeing, then 120,000 × g ultracentrifugation for 70 min (PBS can be used to supplement to the appropriate volume before centrifugation). Discard the supernatant and collect the precipitation, which will be the PKH67-labeled MSC-Exo (avoid light).

Transfection of MSC-Exo and Immunofluorescence

Transfection of MSC-Exo was performed by referring to previous studies.[7,32] PKH67-labeled MSC-Exo and Cy3-labeled miR-138-5p (Guangzhou Ribobio Co., Ltd, Guangzhou, China) were placed on ice for 10 minutes. PKH67-labeled MSC-Exo was resuspended by 400μL PBS and diluted to 0.5mg/mL in electroporation buffer, 2μL of Cy3-labeled miR-138-5p was added at the final concentration of 100nm, and the mixture was transferred to a precooled 2 mm cuvette, 400V, 125μF capacitive pulse, 5ms, 3 pulses. The MSC-Exo after electroporation was placed on ice for 10 min. HSFs (6×10^5 cells/well) stimulated, respectively, with Cy3-labeled miR-138-5p and PKH67-labeled MSC-Exo in the serum-depleted medium for 24 h were fixed with 4% paraformaldehyde. Cells were washed with PBS three times, and nuclear HSFs were stained with 4′,6′-diamidino-2-phenylindole (DAPI; KGA215-10, QIAGEN, Shandong, China) at the concentration of 2μg/mL. The images were observed by an IX81 microscope (Olympus, Tokyo, Japan).

Statistical Analysis

All results were obtained from three independent experiments and expressed as mean ± standard error (SEM). Quantitative data between two groups were analyzed using Student's *t*–test, and two-way analysis of variance (ANOVA) followed by Bonferroni's posttest, which were performed using GraphPad Prism 9.0 software (GraphPad Software, San Diego, CA) or Wilcoxon test was performed using SPSS 26.0 (Statistical Package for the Social Sciences software, IBM Corporation, Armonk, NY, USA). A value of $P < 0.05$ was considered statistically significant.

Results

The Effects of SIRT1 on Biological Behaviors of HSFs

SIRT1 knockdown (KD) and overexpressing (OE) lentivirus were successfully transfected into HSFs (Figure 1A and B). Western blot was used to measure the protein expression level of SIRT1 in control, knockdown NC, knockdown SIRT1, overexpressing negative control (NC), and overexpressing SIRT1 groups (control group was the HSFs without lentivirus transfection, NC group was the HSFs transfected with blank lentivirus). As expected, the protein expression level of SIRT1 was significantly downregulated in the knockdown SIRT1 group compared with the control group and knockdown NC group. On the contrary, the protein expression level of SIRT1 was significantly upregulated in the overexpressing SIRT1 group compared with the control group and overexpressing NC group. The stably infected cells were used for subsequent experiments.

We further verified whether SIRT1 could affect the biological behaviors of HSFs. The proliferation of HSFs in control, knockdown NC, knockdown SIRT1, overexpressing NC, and overexpressing SIRT1 groups were detected by Cell Counting Kit-8 assay. Compared to the control group, SIRT1 knockdown significantly inhibited the proliferation of HSFs, whereas SIRT1 overexpression significantly promoted the proliferation of HSFs (Figure 1C). The migration of HSFs in control, knockdown NC, knockdown SIRT1, overexpressing NC, and overexpressing SIRT1 groups were

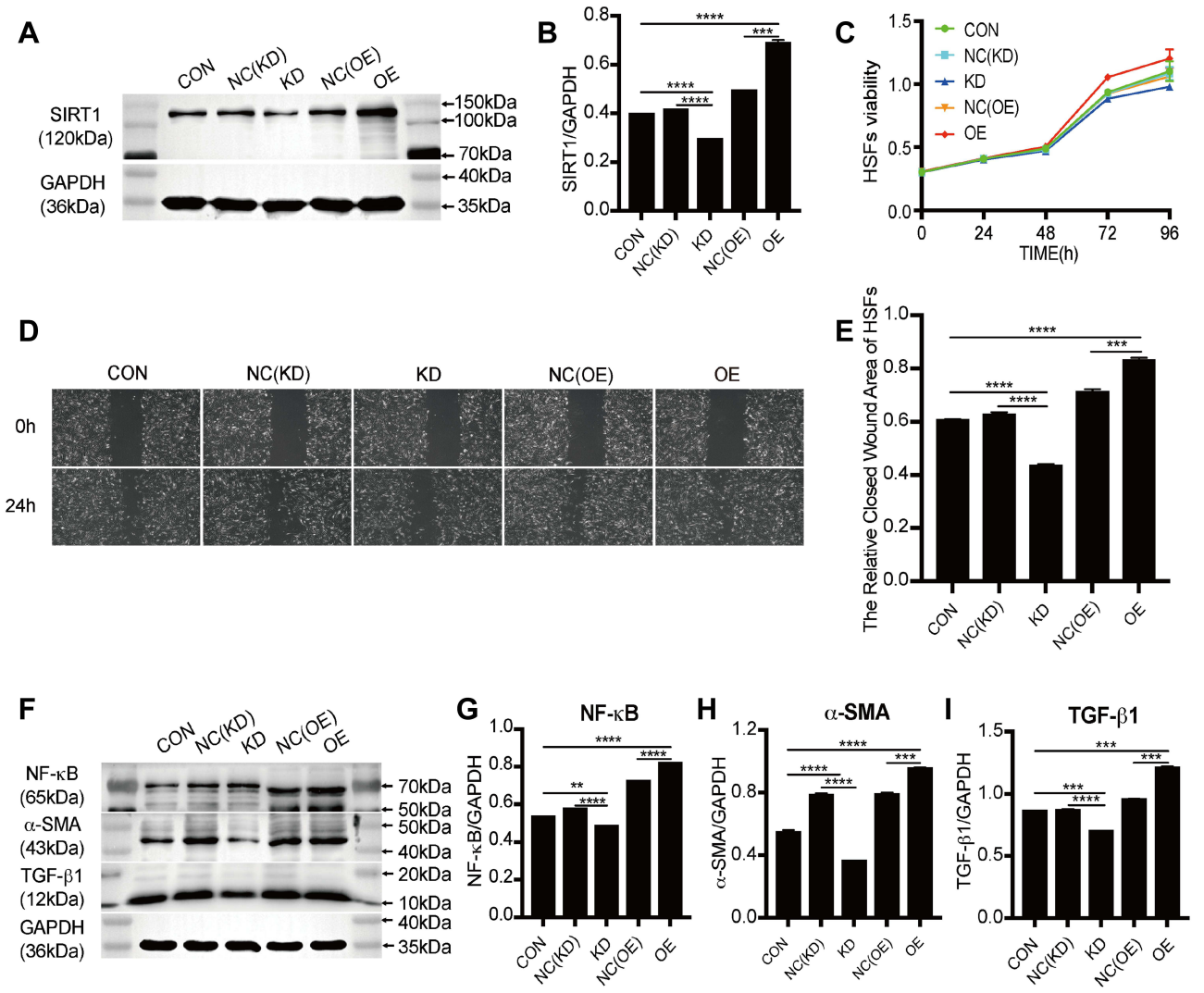

Figure 1 The identification of SIRT1 transfection and the effects of SIRT1 knockdown and overexpression on proliferation, migration and protein expression of HSFs. (**A** and **B**) Western blot analysis of SIRT1 in HSFs transfected with mimic-control, -SIRT1 knockdown, -SIRT1 overexpression and their corresponding negative control for 48h, graph showed the relative band density to GAPDH. (**C**) Cell Counting Kit-8 analysis of the viability of HSFs transfected with mimic-control, -SIRT1 knockdown, -SIRT1 overexpression and their corresponding negative control at 0-, 24-, 48-, 72-, 96h. (**D** and **E**) Scratch analysis of the migration of HSFs transfected with mimic-control, -SIRT1 knockdown, -SIRT1 overexpression and their corresponding negative control at 0-, 24h, graph showed the relative closed wound area of HSFs. (**F–I**) Western blot analysis of NF-κB, α-SMA, and TGF-β1 in HSFs transfected with mimic-control, -SIRT1 knockdown, -SIRT1 overexpression and their corresponding negative control for 48h, graph showed the relative band density to GAPDH. Every experiment was repeated at least three times, the data was shown as mean ± SEM (***P*<0.01, ****P*<0.001, *****P*<0.0001). **Abbreviations**: SIRT1, silent information regulator 1; CON, control; NC, negative control; KD, knockdown; OE, overexpression; NF-κB, nuclear factor-kappa B; α-SMA, α-smooth muscle actin; TGF-β1, transforming growth factor-β1.

detected by scratch and Transwell migration assay. Scratch assay showed that SIRT1 knockdown significantly inhibited the migration of HSFs, whereas SIRT1 overexpression significantly promoted the migration of HSFs (Figure 1D and E). Moreover, the protein expression levels of the NF-κB, α-SMA and TGF-β1 were measured by Western blot. Compared to the control and NC groups, the protein expression levels of NF-κB, α-SMA, and TGF-β1 were significantly upregulated in the overexpressing SIRT1, and NF-κB, α-SMA and TGF-β1 were significantly downregulated in the knockdown SIRT1 (Figure 1F–I). Similarly, the result of Transwell migration assay was consistent with that of scratch assay (Figure 2A and B). Flow cytometry was used to detect the cell cycle and apoptosis of HSFs in control, knockdown NC, knockdown SIRT1, overexpressing NC and overexpressing SIRT1 groups. The result showed that SIRT1 overexpression significantly shortened the cell cycle and inhibited the apoptosis of HSFs (Figure 2C–F). The results of si-SIRT1 in Cell Counting Kit-8 assay, scratch and Transwell migration assay also showed the same effects as they were shown in knockdown SIRT1 (Figure 3A–E). These results

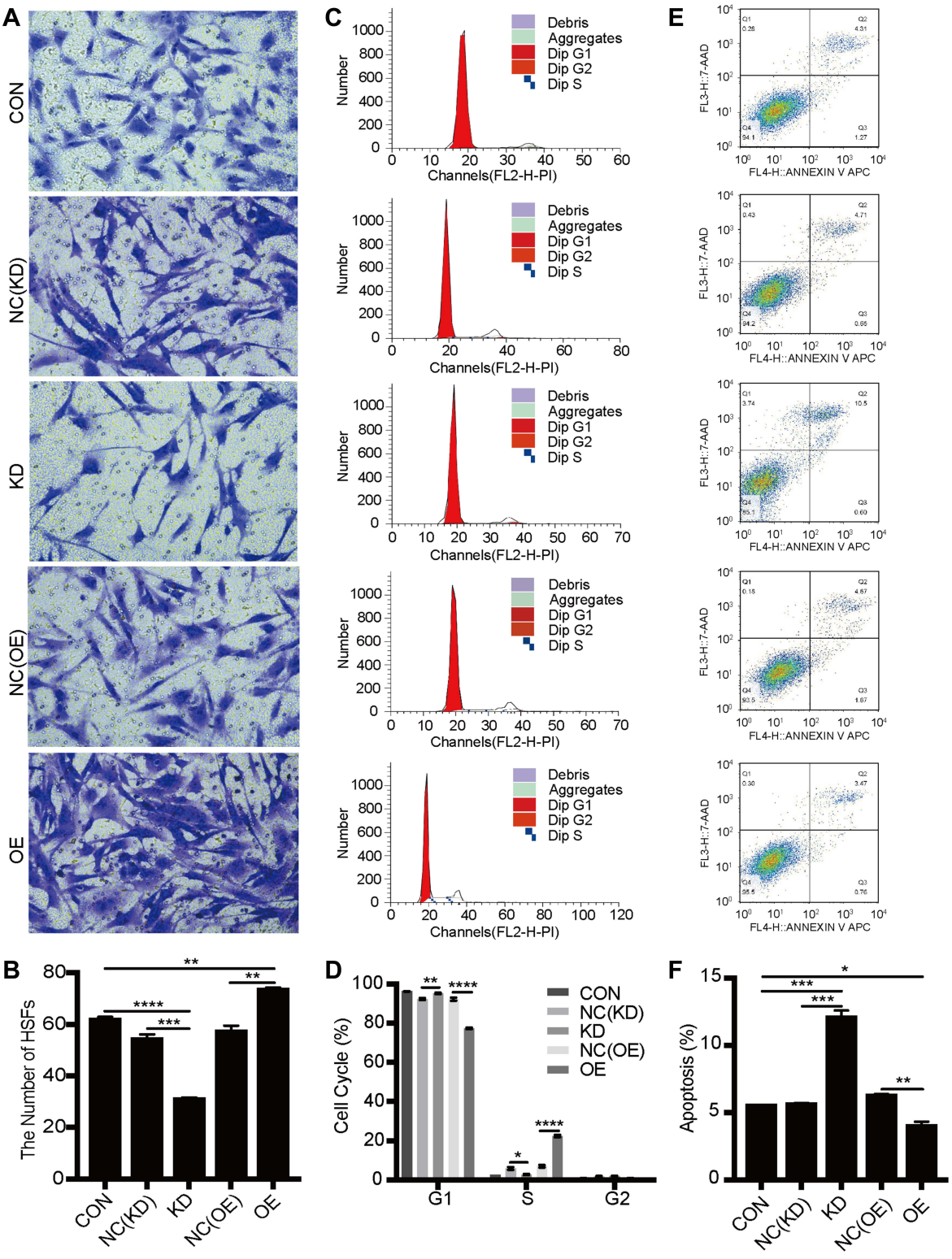

Figure 2 The effects of SIRT1 knockdown and overexpression on migration, cell cycle and apoptosis of HSFs. (**A** and **B**) Transwell migration analysis of the migration of HSFs transfected with mimic-control, -SIRT1 knockdown, -SIRT overexpression and their corresponding negative control for 48h, graph showed the numbers of migrated HSFs. (**C** and **D**) Cell cycle analysis of HSFs transfected with mimic-control, -SIRT1 knockdown NC, -SIRT1 knockdown, -SIRT1 overexpression NC and -SIRT overexpression for 48h. (**E** and **F**) Apoptosis analysis of HSFs transfected with mimic-control, -SIRT1 knockdown NC, -SIRT1 knockdown, -SIRT1 overexpression NC and -SIRT overexpression for 48h, graph showed the proportion of apoptotic HSFs. Every experiment was repeated at least three times, and the data was shown as mean ± SEM (*P<0.05, **P<0.01, ***P<0.001, ****P<0.0001).

Abbreviations: CON, control; NC, negative control; KD, knockdown; OE, overexpression; HSFs, human skin fibroblasts.

https://doi.org/10.2147/IJN.S377317 DovePress

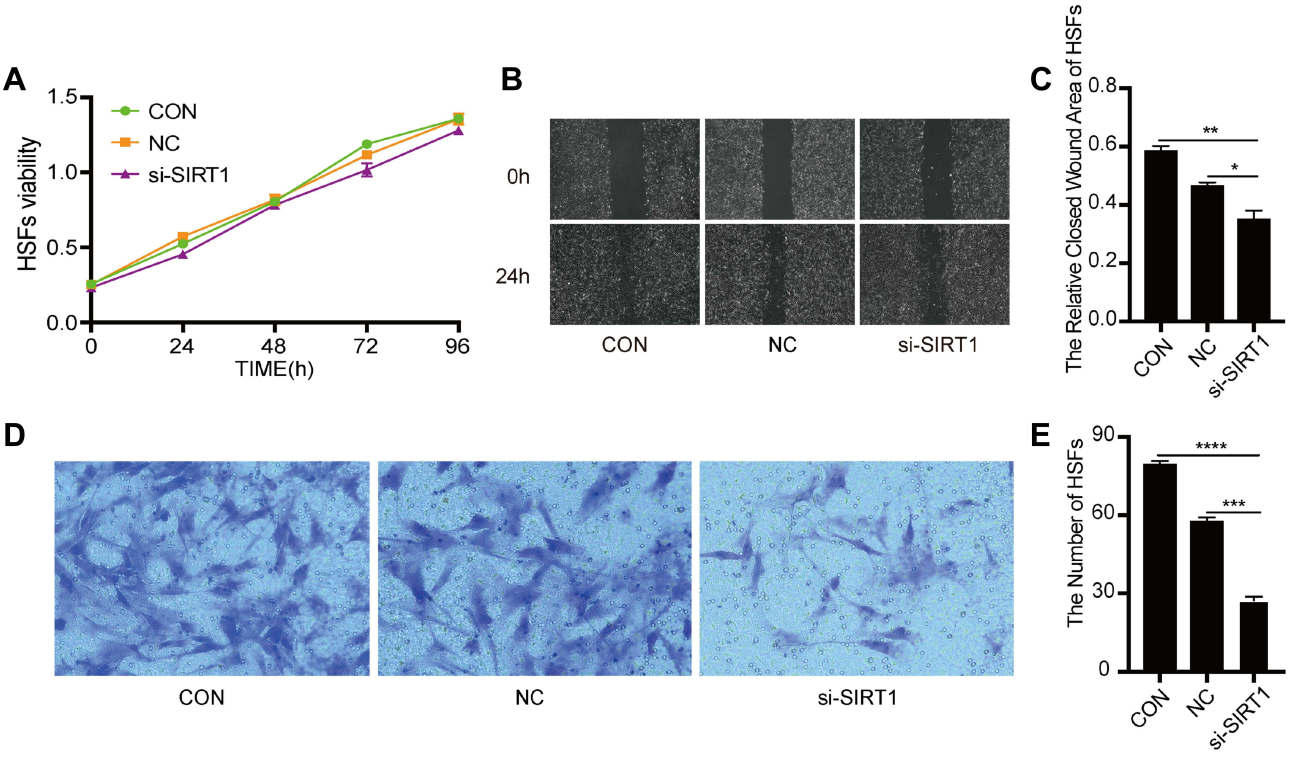

Figure 3 The effect of si-SIRT1 on proliferation and migration of HSFs. (**A**) Cell Counting Kit-8 analysis of the viability of HSFs treated with PBS, SIRT1 siRNA and its negative control at 0-, 24-, 48-, 72-, 96h. (**B** and **C**) Scratch analysis of the migration of HSFs treated with PBS, SIRT1 siRNA and its negative control at 0-, 24h, graph showed the relative closed wound area of HSFs. (**D** and **E**) Transwell migration analysis of the migration of HSFs treated with PBS, SIRT1 siRNA and its negative control for 48h, graph showed the numbers of migrated HSFs. Every experiment was repeated at least three times, and the data was shown as mean ± SEM (*P<0.05, **P<0.01, ***P<0.001, ****P<0.0001).

Abbreviations: HSFs, human skin fibroblasts; CON, control; NC, negative control; si-SIRT1, small interfering-silent information regulator 1.

suggested that SIRT1 promotes proliferation and migration, shortens the cell cycle and inhibits the apoptosis of HSFs, which also increases the inflammatory and profibrotic protein expression, including NF-κB, α-SMA, and TGF-β1, in HSFs.

The Selection of miRNAs That are Both Involved in Regulating SIRT1 and Cell Migration

The miRNAs both involved in regulating SIRT1 and cell migration were firstly selected by miR Walk 2.0 database and literature searching. As a result, hsa-miR-138-5p, hsa-miR-181a-5p, hsa-miR-524-5p, hsa-miR-601 and hsa-miR-1283 were selected out. Subsequently, mimic-NC, -hsa-miR-138-5p, -hsa-miR-181a-5p, -hsa-miR-524-5p, -hsa-miR-601 and -hsa-miR-1283 were successfully transfected into HSFs. Western blot was used to measure the protein expression level of SIRT1 in NC, miR-138-5p, miR-181a-5p, miR-524-5p, miR-601 and miR-1283 groups. The result showed that the protein expression level of SIRT1 was significantly downregulated in the miR-138-5p group compared with the NC group, whereas the protein expression level of SIRT1 was significantly upregulated in the miR-181a-5p, miR-524-5p and miR-601 groups, but miR-1283 showed no significance (Figure 4A and B). Transwell migration assay was used to detect the migration ability of HSFs transfected with different miRNAs, which showed that miR-138-5p and miR-181a-5p significantly inhibited the migration of HSFs compared with NC group, whereas miR-524-5p and miR-1283 significantly promoted the migration of HSFs, but miR-601 showed no significance (Figure 4C and D). Eventually, miR-138-5p was chosen for subsequent experiments, which both significantly downregulate SIRT1 and inhibit HSFs migration.

We further verified whether miR-138-5p could bond to the target site, 3′-UTR, of SIRT1. Mimic-miR-138-5p was transfected into HSFs, and transfected mimic-NC was set as the control group. Then, a dual-luciferase assay was used to

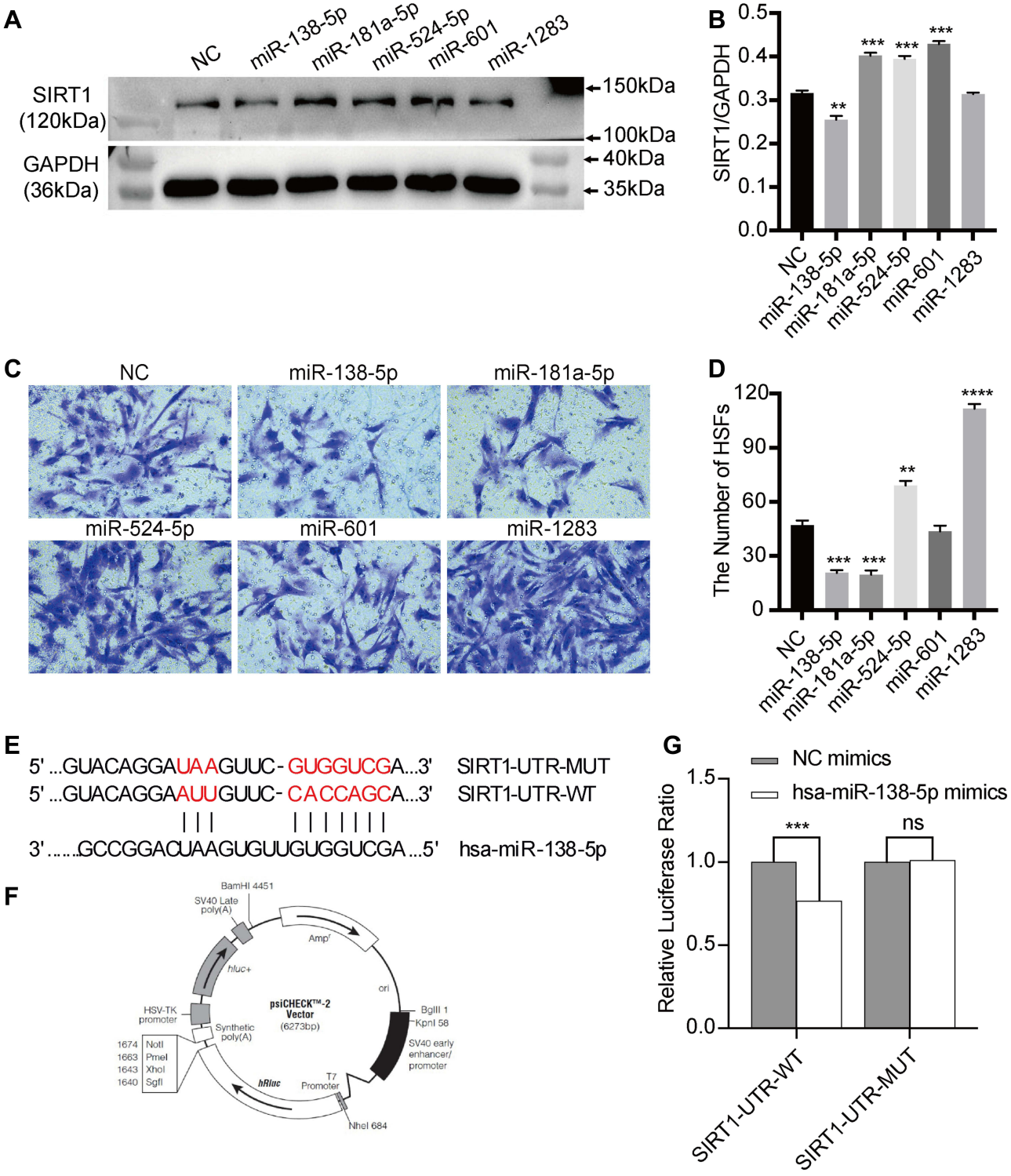

Figure 4 The effects of miRNAs on protein expression of SIRT1 in HSFs and the migration of HSFs, and the verification of the targeted regulatory relationship between miR-138-5p and SIRT1 in HSFs. (**A** and **B**) Western blot analysis of protein expression of SIRT1 in HSFs exposed to miRNAs mimics or mimics NC for 48h, graph showed their levels relative to that of GAPDH. (**C** and **D**) Transwell migration analysis of the migration of HSFs exposed to miRNAs mimics or mimics NC for 48h, graph showed the numbers of migrated HSFs. (**E**) The binding sites predicted by bioinformatics algorithms. (**F** and **G**) The targeted modulation measured by luciferase reporter gene assays. Every experiment was repeated at least three times, and the data was shown as mean ± SEM (***P*<0.01, ****P*<0.001, *****P*<0.0001, ns: no difference).
Abbreviations: SIRT1, silent information regulator 1; NC, negative control; HSFs, human skin fibroblasts; UTR, untranslated regions; WT, wild-type; MUT, mutant-type.

detect the combination. The result showed that luciferase activity in the mimic-miR-138-5p group was reduced to 76.72% of the control group (Figure 4E–G). However, after the predicted target site of SIRT1 was mutated, the activity of luciferase of the mimic-miR-138-5p group was returned to 101.24% of the control group (Figure 4E–G). The result suggested that miR-138-5p could directly bond to the 3′-UTR of SIRT1.

The Effects of MSC-Exo Loaded miR-138-5p on Biological Behaviors of HSFs

The exosomes were isolated from MSCs by ultracentrifugation. The appearance of exosomes observed through a transmission electron microscope (TEM) presented as saucer-like bilayer vesicles (Figure 5A). Nanoparticle tracking analysis was used to detect the size of exosomes, which showed that the peak analysis of exosomes was 145.9nm, which matched the size of exosomes (30–150nm) (Figure 5B). In addition, Western blot was used to detect the protein expression of marker proteins for exosomes, which showed that CD9, CD81, and TSG101 were positively expressed (Figure 5C). These results suggest that exosomes were isolated successfully from MSCs. Subsequently, Cy3-labeled miR-138-5p was transferred into PKH67-labeled MSC-Exo by electroporation. Then, the transfected MSC-Exo and HSFs were co-incubated for 24 hours. The immunofluorescence result showed that PKH67-labeled MSC-Exo carried with Cy3-labeled miR-138-5p successfully transferred into HSFs (Figure 5D).

We further verified whether the miR-138-5p loaded in MSC-Exo could affect the biological behaviors of HSFs. The proliferation of HSFs in control, negative control-exosomes (NC-EXO), and miR-138-5p-exosomes (miR-138-5p-EXO) were detected by Cell Counting Kit-8 assay. miR-138-5p loaded in MSC-Exo inhibited the proliferation of HSFs compared with the control and NC groups (Figure 6A), whereas, after miR-138-5p was inhibited by its inhibitor, the proliferation of HSFs increased (Figure 6B). The migration of HSFs in control, NC-EXO, and miR-138-5p-EXO groups were measured by Transwell migration assay. The result showed that miR-138-5p loaded in MSC-Exo significantly inhibited the migration of HSFs compared with the control and NC groups (Figure 6C and D). However, when miR-138-

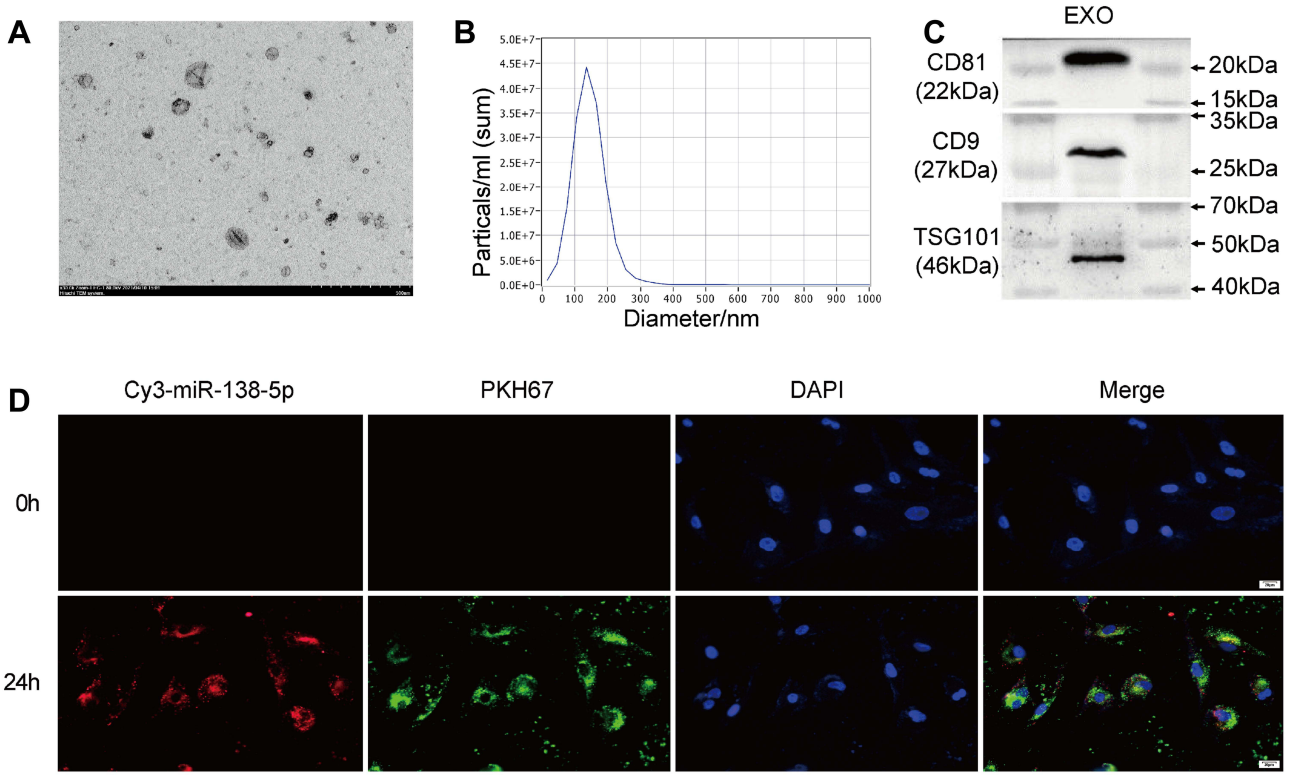

Figure 5 The identification of exosomes derived from mesenchymal stem cells (MSC-Exos). (**A**) The morphology of MSC-Exos analyzed by TEM, scale bar = 500 nm. (**B**) The particle size distribution of MSC-Exos measured by NTA showed that most of the MSC-Exos were 145.9nm in diameter. (**C**) Immunoblot analysis of known exosomal markers (CD81, CD9 and TSG101). (**D**) Representative images of the internalization of PKH67-labeled MSC-Exos containing Cy3-labeled miR-138-5p into HSFs, scale bars = 20 μm. EXO, exosome.

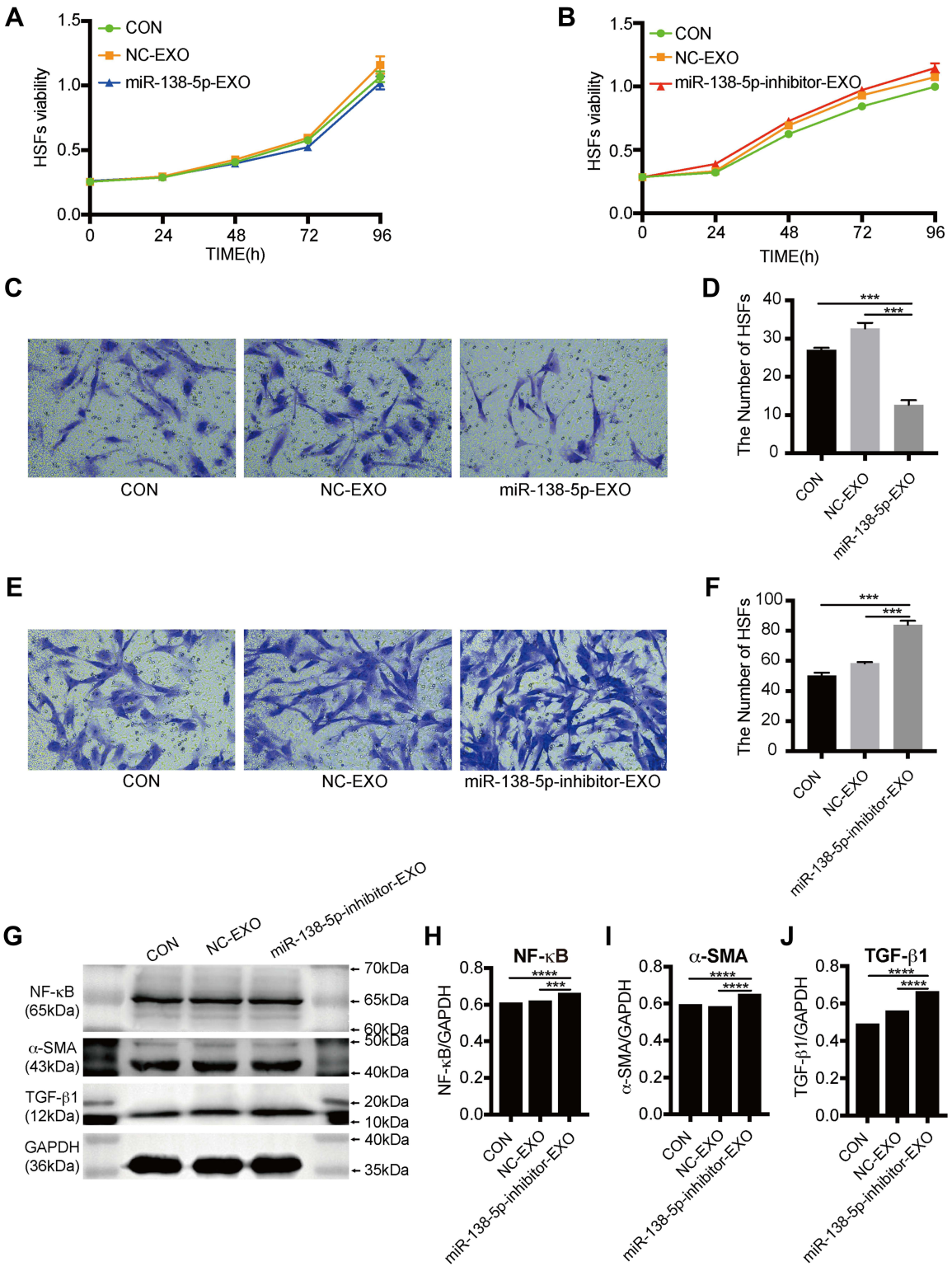

Figure 6 The effect of miR-138-5p on proliferation, migration and protein expression of HSFs. (**A**) Cell Counting Kit-8 analysis of the viability of HSFs stimulated with PBS, MSC-Exos negative control, MSC-Exos containing miR-138-5p at 0-, 24-, 48-, 72-, 96h. (**B**) Cell Counting Kit-8 analysis of the viability of HSFs stimulated with PBS, MSC-Exos negative control, MSC-Exos containing miR-138-5p inhibitor at 0-, 24-, 48-, 72-, 96h. (**C** and **D**) Transwell migration analysis of the migration of HSFs stimulated with PBS, MSC-Exos negative control, MSC-Exos containing miR-138-5p for 48h, graph showed the numbers of migrated HSFs. (**E** and **F**) Transwell migration analysis of the migration of HSFs stimulated with PBS, MSC-Exos negative control, MSC-Exos containing miR-138-5p inhibitor for 48h, graph showed the numbers of migrated HSFs. (**G–J**) Western blot analysis of NF-κB, α-SMA, and TGF-β1 in HSFs stimulated with PBS, MSC-Exos negative control, MSC-Exos containing miR-138-5p inhibitor for 48h, graph showed the relative band density to GAPDH. Every experiment was repeated at least three times, and the data was shown as mean ± SEM (****P*<0.001, *****P*<0.0001).
Abbreviations: HSFs, human skin fibroblasts; CON, control; NC, negative control; EXO, exosome; NF-κB, nuclear factor-kappa B; α-SMA, α-smooth muscle actin; TGF-β1, transforming growth factor-β1.

5p was inhibited by its inhibitor, the migration of HSFs was significantly promoted (Figure 6E and F). These results suggested that miR-138-5p loaded in MSC-Exo inhibit the proliferation and migration of HSFs. Finally, Western blot was used to measure the protein expression level of NF-κB, α-SMA, and TGF-β1. After miR-138-5p was inhibited, the expression of NF-κB, α-SMA and TGF-β1 was significantly upregulated compared with the control and NC groups (Figure 6G–J). The result indicated that miR-138-5p loaded in MSC-Exo decreases the expression of inflammatory and profibrotic proteins, including NF-κB, α-SMA and TGF-β1, which were derived from HSFs.

Discussion

Pathological scars are fibroproliferative disorders of the skin, caused by the high proliferation of fibroblasts, excessive deposition of collagen in the extracellular matrix, and increased response of various immune cells, which not only affects aesthetics but also causes pain, itching, burning, paresthesia, scar contracture and other complications.[33,34] Therefore, effective therapeutics for pathological scars are needed urgently. Our present study firstly demonstrated that the over-expression of SIRT1 gene could promote the biological behaviors of HSFs and may result in scar formation. We also explored the corresponding therapeutics that MSC-Exo could inhibit these processes by downregulating the SIRT1 gene via miR-138-5p.

As a silent signal, it had been identified that SIRT1 could inhibit the biological activities of several cell types and then perform the actions of anti-fibrosis and anti-cancer.[35–37] A previous study demonstrated that the activator of SIRT1 could down-regulate the expression of TNF-α, NF-κB, α-SMA and TGF-β content, then against hepatic fibrosis by activation of SIRT1.[28] Besides, SIRT1 could also ameliorate liver fibrosis by promoting stellate cell apoptosis.[29] On the contrary, another previous study identified that the activation of sirtuin 1, the protein encoded by SIRT1 gene, could elevate transcription of TGF-β target genes and enhance the release of collagen in fibroblasts of systemic sclerosis (SSc), whereas knockdown of sirtuin 1 could effectively inhibit TGF-β signaling and exert potent antifibrotic effects, thus sirtuin1 may be a key regulator of fibroblast activation in SSc.[38] In order to understand the exact effects of SIRT1 in HSFs and then pathological scars, we investigated the effects of SIRT1 on the biological behaviors of HSFs. Our results showed that SIRT1 could promote proliferation and migration of HSFs, shorten the cell cycle of HSFs, and inhibit apoptosis of HSFs, whilst these effects could be reversed by SIRT1 knockdown or si-SIRT1 (Figures 1–3). We also investigated the effects of SIRT1 on protein expression in HSFs by measuring the inflammatory and profibrotic protein expression levels, including NF-κB, α-SMA and TGF-β1. As expected, our results showed that SIRT1 overexpression could upregulate the protein expression of HSFs-derived NF-κB, α-SMA and TGF-β1, which could be reversed by SIRT1 knockdown (Figure 1F–I), indicating that SIRT1 could promote the inflammatory and profibrotic protein expression in HSFs.

Recently, MSCs-based therapies have had positive outcomes both in animal models of pathological scars and clinical patients.[5,39–41] The presence of the defined MSCs was proved by research in various organs and tissues such as bone marrow, adipose tissue, skeletal muscles, dental pulp, umbilical blood, liver, kidneys, and lungs.[42,43] MSCs are multipotent cells characterized by long-term self-renewal and by the potential for differentiation into cells of different mesenchymal tissue types such as fibroblasts, osteoblasts, adipocytes, muscle cells, endothelial cells and chondrocytes.[44,45] Furthermore, exosomes are one of the key secretory products of MSCs, resembling the effect of parental MSCs.[46] They can shuttle various proteins, mRNAs and miRNAs to modulate the activities of recipient cells and play important roles in cutaneous wound healing or scar formation.[46–48] Compared with MSCs, MSC-Exo is more convenient to be stored and transported, which could also avoid many risks associated with cell transplantation.[46] Therefore, MSC-Exo-mediated therapy may be safer and more efficient than MSCs transplantation. Li et al[7] reported that exosomes derived from human adipose mesenchymal stem cells (ADSC-Exo) could effectively inhibit the proliferation and migration of HSFs and decrease Col1, Col3, α-SMA, IL-17RA and p-Smad2/p-Smad3 while increasing the levels of SIP1 in HSFs. They also verified that the ADSC-Exo group showed faster wound healing and less collagen deposition in the mice models, indicating that ADSC-Exo could attenuate hypertrophic scar fibrosis. Besides, MSC-Exo is increasingly used as drug delivery vehicles for the treatment of many diseases based on their size and competence to transfer biological materials to recipient cells.[49–51] Shi et al[52] showed that TGF-β-loaded exosomes could accelerate wound healing both in vitro and in vivo. Yan et al[53] proved that miR-31-5p loaded in

milk-derived exosomes achieved higher cell uptake and was able to resist degradation, and also dramatically improved endothelial cell functions in vitro, together with the promotion of angiogenesis and enhanced diabetic wound healing in vivo, which showed the feasibility of milk-derived exosomes as a scalable, biocompatible, and cost-effective delivery system to enhance the bioavailability and efficacy of miRNAs.

Except for exosomes, liposomes, round vesicles with a hydrophilic center and bilayers of amphiphiles, also play a promising role in tissue regeneration.[54] But compared with exosomes, liposomes are actually foreign substances, which are apt to be phagocytosed by the monocyte-macrophage system and poor targeting.[54] Therefore, exosomes have a more substantial degree of bioactivity and immunogenicity than liposomes as they are distinctly chiefly formed by cells, which improve their steadiness in the bloodstream and enhance their absorption potential and medicinal effectiveness.[54] However, there is lacking effective therapeutics for scar attenuation and drug microcarriers. According to the latest research, arabinoxylan and graphene oxide (GO) using the hydrothermal method through cross-linking GO-arabinoxylan and polyvinyl alcohol (PVA) with tetraethyl orthosilicate (TEOS) to get multifunctional composite hydrogels was the novel therapeutics for wound healing and even scar alleviation.[55] Whether exosomes or liposomes combined with such a hydrogel could get better outcomes needs further study.

Moreover, therapies using miRNAs are promising means of regulating the gene expression involved in wound healing and scar formation.[56–58] miRNAs could also exert their work as a modification to MSCs or MSC-Exo, reducing excessive scar formation. As previous studies introduced, the MSCs or MSC-Exo modified by miR-181-5p, miR-29a, miR-146a, miR-21, miR-146a-5p, etc.[10,59–62] showed promising effectiveness of anti-fibrosis and remodeling on alleviating scar formation and accelerated wound healing. Li et al[63] demonstrated that miR-3613-3p inhibited HS formation via targeting arginine and glutamate-rich 1, which may provide potential therapeutic targets for the management of HS. Zhang et al[64] verified that miR-124-3p could inhibit the proliferation of HS fibroblasts by targeting TGF-β1 and may thus be a potential therapeutic target for HS. Shen et al[65] showed that miR-145-5p arrests the development of fibrogenesis and decreases HS formation by reducing the expression of Smad2/3, indicating that miR-145-5p may be an optional novel molecular target for treating HS. However, the advancement of miRNA therapies has been impeded by the lack of an effective delivery method.[20] MSC-Exo has been used to deliver exogenous miRNAs to target cells to address this issue.[19] Meanwhile, we identified that miR-138-5p could inhibit the proliferation and migration of HSFs and downregulate the expression of the inflammatory and profibrotic proteins, such as NF-κB, α-SMA and TGF-β1, by directly targeting to 3′-URT of SIRT1 via MSC-Exo delivery, whereas these effects were significantly reversed by the miR-138-5p inhibitor (Figure 6A–J), which were consistent to our hypothesis and previous study.[24] Therefore, the promising role of miR-138-5p in downregulating SIRT1 inhibits the growth of HSFs, which may be a promising therapeutic for attenuating the formation and development of pathological scars. In addition, the use of MSC-Exo as a delivery vehicle for miR-138-5p transfer into HSFs may be an effective way to enhance the effects of miR-138-5p.

Here, we described a process by which MSC-Exo containing miR-138-5p regulates proliferation and migration of HSFs and the expression levels of downstream inflammatory and profibrotic proteins in HSFs, including NF-κB, α-SMA and TGF-β1. As expected, miR-138-5p could transfer into HSFs delivered by MSC-Exo, then directly bond to 3′-UTR of SIRT1, then perform as inhibiting the proliferation, migration and protein expression of HSFs.

Conclusion

In conclusion, knockdown of SIRT1 inhibited the proliferation and migration of HSFs, indicating that SIRT1 may be the target gene to alleviate pathological scars. Meanwhile, exosomes derived from MSCs could inhibit the proliferation and migration of HSFs by downregulating SIRT1 via miR-138-5p in vitro, which may be a therapeutic option for pathological scars. Therefore, exosomes derived from MSCs may be an effective way to deliver miR-138-5p and inhibit the growth and protein expression of HSFs, then attenuate pathological scars.

Acknowledgments

Thanks to the funding of the National Natural Science Foundation of China (81901968), the Provincial Natural Science Foundation of Shandong province (ZR2019BH051) and the Postdoctoral Science Foundation of China (2018M642667). Special thanks to Dr. Nan Liu for pre-reviewing our manuscript.

Funding

This study was financially supported by the National Natural Science Foundation of China (81901968), the Provincial Natural Science Foundation of Shandong province (ZR2019BH051) and the Postdoctoral Science Foundation of China (2018M642667).

Disclosure

The authors report no conflicts of interest in this work.

References

1. Lee HJ, Jang YJ. Recent understandings of biology, prophylaxis and treatment strategies for hypertrophic scars and keloids. *Int J Mol Sci*. 2018;19(3):711. doi:10.3390/ijms19030711
2. Ogawa R. Keloid and hypertrophic scars are the result of chronic inflammation in the reticular dermis. *Int J Mol Sci*. 2017;18(3):606. doi:10.3390/ijms18030606
3. Jiang D, Christ S, Correa-Gallegos D, et al. Injury triggers fascia fibroblast collective cell migration to drive scar formation through N-cadherin. *Nat Commun*. 2020;11(1):5653. doi:10.1038/s41467-020-19425-1
4. Wang ZC, Zhao WY, Cao Y, et al. The roles of inflammation in keloid and hypertrophic scars. *Front Immunol*. 2020;11:603187. doi:10.3389/fimmu.2020.603187
5. Casado-Díaz A, Quesada-Gómez JM, Dorado G. Extracellular vesicles derived from mesenchymal stem cells (MSC) in regenerative medicine: applications in skin wound healing. *Front Bioeng Biotechnol*. 2020;8:146. doi:10.3389/fbioe.2020.00146
6. Wu D, Kang L, Tian J, et al. Exosomes derived from bone mesenchymal stem cells with the stimulation of Fe3O4 nanoparticles and static magnetic field enhance wound healing through upregulated miR-21-5p. *Int J Nanomedicine*. 2020;15:7979–7993. doi:10.2147/ijn.S275650
7. Li Y, Zhang J, Shi J, et al. Exosomes derived from human adipose mesenchymal stem cells attenuate hypertrophic scar fibrosis by miR-192-5p/IL-17RA/Smad axis. *Stem Cell Res Ther*. 2021;12(1):221. doi:10.1186/s13287-021-02290-0
8. An Y, Lin S, Tan X, et al. Exosomes from adipose-derived stem cells and application to skin wound healing. *Cell Prolif*. 2021;54(3):e12993. doi:10.1111/cpr.12993
9. Kalluri R, LeBleu VS. The biology, function, and biomedical applications of exosomes. *Science*. 2020;367(6478):eaau6977. doi:10.1126/science.aau6977
10. Yuan R, Dai X, Li Y, Li C, Liu L. Exosomes from miR-29a-modified adipose-derived mesenchymal stem cells reduce excessive scar formation by inhibiting TGF-β2/Smad3 signaling. *Mol Med Rep*. 2021;24(5):758. doi:10.3892/mmr.2021.12398
11. Ha DH, Kim HK, Lee J, et al. Mesenchymal stem/stromal cell-derived exosomes for immunomodulatory therapeutics and skin regeneration. *Cells*. 2020;9(5):1157. doi:10.3390/cells9051157
12. Fang S, Xu C, Zhang Y, et al. Umbilical cord-derived mesenchymal stem cell-derived exosomal MicroRNAs suppress myofibroblast differentiation by inhibiting the transforming growth factor-β/SMAD2 pathway during wound healing. *Stem Cells Transl Med*. 2016;5(10):1425–1439. doi:10.5966/sctm.2015-0367
13. Bian D, Wu Y, Song G, Azizi R, Zamani A. The application of mesenchymal stromal cells (MSCs) and their derivative exosome in skin wound healing: a comprehensive review. *Stem Cell Res Ther*. 2022;13(1):24. doi:10.1186/s13287-021-02697-9
14. Lu TX, Rothenberg ME. MicroRNA. *J Allergy Clin Immunol*. 2018;141(4):1202–1207. doi:10.1016/j.jaci.2017.08.034
15. Stavast CJ, Erkeland SJ. The non-canonical aspects of MicroRNAs: many roads to gene regulation. *Cells*. 2019;8(11):1465. doi:10.3390/cells8111465
16. He T, Zhang Y, Liu Y, et al. MicroRNA-494 targets PTEN and suppresses PI3K/AKT pathway to alleviate hypertrophic scar formation. *J Mol Histol*. 2019;50(4):315–323. doi:10.1007/s10735-019-09828-w
17. Shi Y, Wang L, Yu P, Liu Y, Chen W. MicroRNA-486-5p inhibits the growth of human hypertrophic scar fibroblasts by regulating Smad2 expression. *Mol Med Rep*. 2019;19(6):5203–5210. doi:10.3892/mmr.2019.10186
18. Zhou Y, Shi X, Li S, Gan Q, Cui Z. microRNA-181a promotes the proliferation of hypertrophic scar fibroblasts and inhibits their apoptosis via targeting phosphatase and tensin homolog. *Ann Palliat Med*. 2021;10(4):4563–4571. doi:10.21037/apm-21-604
19. Meng Z, Zhou D, Gao Y, Zeng M, Wang W. miRNA delivery for skin wound healing. *Adv Drug Deliv Rev*. 2018;129:308–318. doi:10.1016/j.addr.2017.12.011
20. Babalola O, Mamalis A, Lev-Tov H, Jagdeo J. The role of microRNAs in skin fibrosis. *Arch Dermatol Res*. 2013;305(9):763–776. doi:10.1007/s00403-013-1410-1
21. Zhang D, Liu X, Zhang Q, Chen X. miR-138-5p inhibits the malignant progression of prostate cancer by targeting FOXC1. *Cancer Cell Int*. 2020;20:297. doi:10.1186/s12935-020-01386-6
22. Zhang W, Liao K, Liu D. MiR-138-5p inhibits the proliferation of gastric cancer cells by targeting DEK. *Cancer Manag Res*. 2020;12:8137–8147. doi:10.2147/cmar.S253777
23. Tarazón E, de Unamuno Bustos B, Murria Estal R, et al. MiR-138-5p suppresses cell growth and migration in melanoma by targeting telomerase reverse transcriptase. *Genes*. 2021;12(12):1931. doi:10.3390/genes12121931
24. Yang D, Li M, Du N. Effects of the circ_101238/miR-138-5p/CDK6 axis on proliferation and apoptosis keloid fibroblasts. *Exp Ther Med*. 2020;20(3):1995–2002. doi:10.3892/etm.2020.8917
25. Zhang J, Peng J, Kong D, et al. Silent information regulator 1 suppresses epithelial-to-mesenchymal transition in lung cancer cells via its regulation of mitochondria status. *Life Sci*. 2021;280:119716. doi:10.1016/j.lfs.2021.119716
26. Singh V, Ubaid S. Role of Silent Information Regulator 1 (SIRT1) in regulating oxidative stress and inflammation. *Inflammation*. 2020;43(5):1589–1598. doi:10.1007/s10753-020-01242-9
27. Wang Y, Wang J, Liu C, Li M. Silent information regulator 1 promotes proliferation, migration, and invasion of cervical cancer cells and is upregulated by human papillomavirus 16 E7 oncoprotein. *Gynecol Obstet Invest*. 2022;87(1):22–29. doi:10.1159/000520642

28. Abd El Motteleb DM, Ibrahim I, Elshazly SM. Sildenafil protects against bile duct ligation induced hepatic fibrosis in rats: potential role for silent information regulator 1 (SIRT1). *Toxicol Appl Pharmacol*. 2017;335:64–71. doi:10.1016/j.taap.2017.09.021
29. Wu Y, Liu X, Zhou Q, et al. Silent information regulator 1 (SIRT1) ameliorates liver fibrosis via promoting activated stellate cell apoptosis and reversion. *Toxicol Appl Pharmacol*. 2015;289(2):163–176. doi:10.1016/j.taap.2015.09.028
30. Tu L, Lin Z, Huang Q, Liu D. USP15 enhances the proliferation, migration, and collagen deposition of hypertrophic scar-derived fibroblasts by deubiquitinating TGF-βR1 in vitro. *Plast Reconstr Surg*. 2021;148(5):1040–1051. doi:10.1097/prs.0000000000008488
31. Zhao D, Wang Y, Du C, et al. Honokiol alleviates hypertrophic scar by targeting transforming growth factor-β/Smad2/3 signaling pathway. *Front Pharmacol*. 2017;8:206. doi:10.3389/fphar.2017.00206
32. Qiu X, Liu J, Zheng C, et al. Exosomes released from educated mesenchymal stem cells accelerate cutaneous wound healing via promoting angiogenesis. *Cell Prolif*. 2020;53(8):e12830. doi:10.1111/cpr.12830
33. Huang C, Ogawa R. Systemic factors that shape cutaneous pathological scarring. *FASEB j*. 2020;34(10):13171–13184. doi:10.1096/fj.202001157R
34. Griffin MF, desJardins-Park HE, Mascharak S, Borrelli MR, Longaker MT. Understanding the impact of fibroblast heterogeneity on skin fibrosis. *Dis Model Mech*. 2020;13(6):dmm044164. doi:10.1242/dmm.044164
35. Liu ZH, Zhang Y, Wang X, et al. SIRT1 activation attenuates cardiac fibrosis by endothelial-to-mesenchymal transition. *Biomed Pharmacother*. 2019;118:109227. doi:10.1016/j.biopha.2019.109227
36. Li P, Liu Y, Qin X, et al. SIRT1 attenuates renal fibrosis by repressing HIF-2α. *Cell Death Discov*. 2021;7(1):59. doi:10.1038/s41420-021-00443-x
37. Zhang S, Yang Y, Huang S, et al. SIRT1 inhibits gastric cancer proliferation and metastasis via STAT3/MMP-13 signaling. *J Cell Physiol*. 2019;234 (9):15395–15406. doi:10.1002/jcp.28186
38. Zerr P, Palumbo-Zerr K, Huang J, et al. Sirt1 regulates canonical TGF-β signalling to control fibroblast activation and tissue fibrosis. *Ann Rheum Dis*. 2016;75(1):226–233. doi:10.1136/annrheumdis-2014-205740
39. Bojanic C, To K, Hatoum A, et al. Mesenchymal stem cell therapy in hypertrophic and keloid scars. *Cell Tissue Res*. 2021;383(3):915–930. doi:10.1007/s00441-020-03361-z
40. Sierra-Sánchez Á, Montero-Vilchez T, Quiñones-Vico MI, Sanchez-Diaz M, Arias-Santiago S. Current advanced therapies based on human mesenchymal stem cells for skin diseases. *Front Cell Dev Biol*. 2021;9:643125. doi:10.3389/fcell.2021.643125
41. Naji A, Eitoku M, Favier B, Deschaseaux F, Rouas-Freiss N, Suganuma N. Biological functions of mesenchymal stem cells and clinical implications. *Cell Mol Life Sci*. 2019;76(17):3323–3348. doi:10.1007/s00018-019-03125-1
42. Lv FJ, Tuan RS, Cheung KM, Leung VY. Concise review: the surface markers and identity of human mesenchymal stem cells. *Stem Cells*. 2014;32 (6):1408–1419. doi:10.1002/stem.1681
43. El Agha E, Kramann R, Schneider RK, et al. Mesenchymal stem cells in fibrotic disease. *Cell Stem Cell*. 2017;21(2):166–177. doi:10.1016/j.stem.2017.07.011
44. Keshtkar S, Azarpira N, Ghahremani MH. Mesenchymal stem cell-derived extracellular vesicles: novel frontiers in regenerative medicine. *Stem Cell Res Ther*. 2018;9(1):63. doi:10.1186/s13287-018-0791-7
45. Ji K, Ding L, Chen X, et al. Mesenchymal stem cells differentiation: mitochondria matter in osteogenesis or adipogenesis direction. *Curr Stem Cell Res Ther*. 2020;15(7):602–606. doi:10.2174/1574888x15666200324165655
46. Phinney DG, Pittenger MF. Concise review: MSC-derived exosomes for cell-free therapy. *Stem Cells*. 2017;35(4):851–858. doi:10.1002/stem.2575
47. Wu P, Zhang B, Shi H, Qian H, Xu W. MSC-exosome: a novel cell-free therapy for cutaneous regeneration. *Cytotherapy*. 2018;20(3):291–301. doi:10.1016/j.jcyt.2017.11.002
48. Toh WS, Lai RC, Zhang B, Lim SK. MSC exosome works through a protein-based mechanism of action. *Biochem Soc Trans*. 2018;46(4):843–853. doi:10.1042/bst20180079
49. Xunian Z, Kalluri R. Biology and therapeutic potential of mesenchymal stem cell-derived exosomes. *Cancer Sci*. 2020;111(9):3100–3110. doi:10.1111/cas.14563
50. Mendt M, Rezvani K, Shpall E. Mesenchymal stem cell-derived exosomes for clinical use. *Bone Marrow Transplant*. 2019;54(Suppl 2):789–792. doi:10.1038/s41409-019-0616-z
51. Zhao T, Sun F, Liu J, et al. Emerging role of mesenchymal stem cell-derived exosomes in regenerative medicine. *Curr Stem Cell Res Ther*. 2019;14 (6):482–494. doi:10.2174/1574888x14666190228103230
52. Shi A, Li J, Qiu X, et al. TGF-β loaded exosome enhances ischemic wound healing in vitro and in vivo. *Theranostics*. 2021;11(13):6616–6631. doi:10.7150/thno.57701
53. Yan C, Chen J, Wang C, et al. Milk exosomes-mediated miR-31-5p delivery accelerates diabetic wound healing through promoting angiogenesis. *Drug Deliv*. 2022;29(1):214–228. doi:10.1080/10717544.2021.2023699
54. Shafiei M, Ansari MNM, Razak SIA, Khan MUA. A comprehensive review on the applications of exosomes and liposomes in regenerative medicine and tissue engineering. *Polymers*. 2021;13(15):2529. doi:10.3390/polym13152529
55. Khan MUA, Razak SIA, Hassan A, Qureshi S, Stojanović GM, Ihsan UH. Multifunctional arabinoxylan-functionalized-graphene oxide based composite hydrogel for skin tissue engineering. *Front Bioeng Biotechnol*. 2022;10:865059. doi:10.3389/fbioe.2022.865059
56. Hu Y, Rao SS, Wang ZX, et al. Exosomes from human umbilical cord blood accelerate cutaneous wound healing through miR-21-3p-mediated promotion of angiogenesis and fibroblast function. *Theranostics*. 2018;8(1):169–184. doi:10.7150/thno.21234
57. Gu S, Huang X, Xu X, et al. Inhibition of CUB and sushi multiple domains 1 (CSMD1) expression by miRNA-190a-3p enhances hypertrophic scar-derived fibroblast migration in vitro. *BMC Genomics*. 2021;22(1):613. doi:10.1186/s12864-021-07920-8
58. Zhang Z, Huang X, Yang J, et al. Identification and functional analysis of a three-miRNA ceRNA network in hypertrophic scars. *J Transl Med*. 2021;19(1):451. doi:10.1186/s12967-021-03091-y
59. Qu Y, Zhang Q, Cai X, et al. Exosomes derived from miR-181-5p-modified adipose-derived mesenchymal stem cells prevent liver fibrosis via autophagy activation. *J Cell Mol Med*. 2017;21(10):2491–2502. doi:10.1111/jcmm.13170
60. Chen MG, Wu MY, Zou ML, Zeng MY. Effect of MicroRNA-146a modified adipose-derived stem cell exosomes on rat back wound healing. *Int J Low Extrem Wounds*. 2021. doi:10.1177/15347346211038092
61. Li Q, Fang L, Chen J, et al. Exosomal MicroRNA-21 promotes keloid fibroblast proliferation and collagen production by inhibiting Smad7. *J Burn Care Res*. 2021;42(6):1266–1274. doi:10.1093/jbcr/irab116

62. Wgealla M, Liang H, Chen R, et al. Amniotic fluid derived stem cells promote skin regeneration and alleviate scar formation through exosomal miRNA-146a-5p via targeting CXCR4. *J Cosmet Dermatol*. 2022. doi:10.1111/jocd.14956
63. Li L, Han W, Chen Y, Chen Y. MiR-3613-3p inhibits hypertrophic scar formation by down-regulating arginine and glutamate-rich 1. *Mol Cell Biochem*. 2021;476(2):1025–1036. doi:10.1007/s11010-020-03968-4
64. Zhang S, Pan S. miR-124-3p targeting of TGF-β1 inhibits the proliferation of hypertrophic scar fibroblasts. *Adv Clin Exp Med*. 2021;30 (3):263–271. doi:10.17219/acem/131753
65. Shen W, Wang Y, Wang D, Zhou H, Zhang H, Li L. miR-145-5p attenuates hypertrophic scar via reducing Smad2/Smad3 expression. *Biochem Biophys Res Commun*. 2020;521(4):1042–1048. doi:10.1016/j.bbrc.2019.11.040